Experimental Investigation of Vinyl Chloride Polymerization at High Conversion—Conversion and Tracer Response Relationships

T. Y. XIE, A. E. HAMIELEC,* P. E. WOOD, and D. R. WOODS, *Department of Chemical Engineering, Institute for Polymer Production Technology (MIPPT), McMaster University, Hamilton, Ontario, Canada L8S 4L7,* and H. WESTMIJZE, *Research Center Deventer, AKZO Chemicals BV, Emmastraat 33, P.O. Box 10, 7400 AA Deventer, The Netherlands*

Synopsis

A model for suspension polymerization which relates the conversion of vinyl chloride monomer (VCM) to polymerization conditions and a tracer response measured by online gas chromatography has been developed. This model can be used to determine monomer conversion with measurements of tracer response by gas chromatograph. A series of experiments using inert mixtures of H_2O/PVC/VCM/*n*-butane and using suspension polymerization of VCM with *n*-butane as tracer were carried out to evaluate the model. The solubility of *n*-butane in vinyl chloride was determined in the temperature range 40–70°C. The solubility of *n*-butane in polyvinylchloride (PVC) was estimated using nonlinear regression comparing model and experimental data for both inert mixtures and for suspension polymerization. Correlations of the solubility constants of *n*-butane in VCM and PVC, respectively, were obtained from the experimental data. Under the present experimental conditions, conversions can be measured online every 7–8 min using the *n*-butane tracer method.

INTRODUCTION

Conversion measurements for polymerization can be classified as direct and indirect methods; the former analyzes the mass of monomer or polymer directly, and the latter measures a property change of the polymerization system which relates to the mass of monomer or polymer formed. Most conversion monitoring techniques are difficult to apply to the suspension polymerization of VCM due to the mechanical difficulties in handling the heterogeneous mixture of water, monomer, and polymer particles of various size at high pressure. The most common method for conversion measurements of VCM polymerization on a small scale is gravimetric analysis,[1-5] which is done by the time-consuming operation of loading reactors (glass ampoules, glass bottles, or stainless steel cells), polymerizing for a given time, venting the unreacted monomer, washing, filtering, drying, and weighing the polymer formed. The difficulties and inaccuracies of polymerization times and initiator and monomer uniformity are obvious. Besides, it is very difficult with these experimental operations to avoid exposing the researcher to VCM, a health hazard.[6] Calorimetry, which is not burdened with the above problems, has been used to measure the polymerization rate,[7-10] and is particularly effective with large commercial reactors. The main

* To whom correspondence should be addressed.

Journal of Applied Polymer Science, Vol. 41, 2327–2347 (1990)
© 1990 John Wiley & Sons, Inc. CCC 0021-8995/90/9-102327-21$04.00

limitation of this experimental technique is the effectiveness of the insulation of the reactor to prevent heat losses to the surroundings, and this is an integral technique with errors in heat generation to estimate conversion accumulating. Therefore, the potential for serious error in conversion estimates is great with small reactors.

A novel method which should avoid the above problems is the tracer analysis method. This method involves the use of an internal calibration reference or tracer which is a chemically inert compound. The tracer should have high solubility in monomer and low solubility in water and polymer, and appropriate vapor pressure at the polymerization temperature. The tracer is added to the VCM polymerization system at the beginning of polymerization. With increase in VCM conversion, the concentration of the tracer in the gas phase increases, giving a correlation between conversion and tracer concentration in the gas phase (it can readily be determined online by gas chromatography). Only one paper[11] reported the application of this method to a VCM polymerization system. A comprehensive model which relates conversion to tracer response has not been published to date. The development of a valid model which correlates conversion with tracer response, therefore, is vital for the application of gas chromatography to monitor conversion during VCM polymerization. Hence, the objective of this work is to develop such a valid model which can be used to estimate VCM conversions online during suspension polymerization using tracer responses measured by gas chromatography, and to evaluate the model using a wide range of polymerization conditions.

MODEL DEVELOPMENT

The monomer distribution among phases during VCM suspension polymerization has been described in detail in a previous paper.[12] The present model relates conversion of monomer to polymer as a function of polymerization conditions and tracer response by gas chromatography. In the course of suspension polymerization of VCM, the tracer exists in the vapor, monomer, water, and polymer phases. However, the partition of the tracer between these phases is quite different because the tracer selected should have a high solubility in VCM but low solubilities in water and PVC. During polymerization, the mass of the monomer phase decreases gradually with conversion; thus, the concentration of tracer in the monomer and gas phases increases. Therefore, one should be able to find a relationship between conversion and tracer concentration in the vapour phase.

The model development is based on the following assumptions:

1. The distributions of species among phases are in instantaneous equilibrium over the entire conversion range.
2. The PVT properties of the vapor phase obey the ideal gas law.
3. The solubility of tracer in water, monomer and polymer phase follows Henry's law.
4. The solubility of PVC in the monomer phase is negligible.
5. The solubility of tracer in the monomer is independent of PVC; i.e., both

the free monomer and the monomer swollen in PVC are treated as equivalent when calculating the tracer concentration.

According to these assumptions, we considered both tracer and monomer distributions in the phases of the polymerization system and theoretically derived the following equations. At equilibrium, the fugacities of tracer in the different phases are equal, i.e.,

$$f_g = f_m = f_w = f_p \tag{1}$$

For the ideal gas,

$$f_g = Y_b P \tag{2}$$

According to Henry's law, the fugacities of tracer in monomer, water, and polymer can be written as

$$f_i = K_{bi} X_{bi} \qquad (i = m, w, p) \tag{3}$$

Substituting eq. (2) and (3) into eq. (1), one has

$$Y_b P = K_{bw} X_{bw} = K_{bm} X_{bm} = K_{bp} X_{bp} \tag{4}$$

where X_{bw} and X_{bm} are mole fractions of tracer in the water and monomer, respectively. X_{bp} is the volume fraction of tracer in the polymer.

The total mass balance for the tracer is as follows:

$$B_m + B_p + B_g + B_w = B \tag{5}$$

The mass of tracer in the vapor phase is given by

$$B_g = \frac{PV_g}{RT} Y_b M_b \tag{6}$$

The mass of tracer in the water phase can be expressed as

$$B_w = \frac{W_w P}{M_w K_{bw}} Y_b M_b \tag{7}$$

From eq. (4), one can find B_p as

$$B_p = \frac{K_{bm} B_m M_{vc} M_0 D_b X}{(M_0 - M_0 X - M_g - M_{wi}) M_b K_{bp} D_p} \tag{8}$$

Substituting eqs. (6)–(8) into eq. (5), one gets

$$B_m = \frac{(B - Y_b Q)(M_0 - M_0 X - M_g - M_{wi}) M_b K_{bp} D_p}{(M_0 - M_0 X - M_g M_{wi}) M_b K_{bp} D_p + K_{bm} M_{vc} M_0 D_b X} \tag{9}$$

From eq. (4), Y_b is given by

$$Y_b = \frac{K_{bm}B_m M_{vc}}{P(M_0 - M_0X - M_g - M_{wi})M_b} \tag{10}$$

Combining eqs. (9) and (10), one can obtain

$$Y_b = \frac{K_{bm}M_{vc}K_{bp}D_pB}{P[(M_0 - M_0X - M_g - M_{wi})M_bK_{bp}D_p + K_{bm}M_{vc}M_0X D_b] + QK_{bm}M_{vc}K_{bp}D_p} \tag{11}$$

where

$$Q = \frac{PV_gM_b}{RT} + \frac{W_wPM_b}{M_wK_{bw}} \tag{12}$$

Equation (11) relates the mole fraction of tracer in gas phase to polymerization conditions over the entire conversion range. The initial value of Y_b can be obtained by setting zero conversion in eq. (11), i.e.,

$$Y_{b0} = \frac{K_{bm}M_{vc}K_{bp}D_pB}{P_0(M_0 - M_{g0} - M_{w0})M_bK_{bp}D_p + Q_0K_{bm}M_{vc}K_{bp}D_p} \tag{13}$$

The mole fraction of tracer in the gas phase can be measured by gas chromatography since it is proportional to the area of GC response, i.e.,

$$Y_b = K_bA_b \tag{14}$$

$$Y_{b0} = K_bA_{b0} \tag{15}$$

Hence,

$$Y_b/Y_{b0} = A_b/A_{b0} = A \tag{16}$$

Substituting eqs. (11) and (13) into eq. (16), one can get the following relation between tracer response and conversion:

$$A = \frac{P_0(M_0 - M_{g0} - M_{w0})M_bK_{bp}D_p + Q_0K_{bm}M_{vc}K_{bp}D_p}{P[(M_0 - M_0X - M_g - M_{wi})M_bK_{bp}D_p + K_{bm}M_{vc}M_0X D_b] + QK_{bm}M_{vc}K_{bp}D_p} \tag{17}$$

The advantage in the use of the ratio of tracer response areas instead of tracer response area is that the instrumental constant K_b and the total mass of tracer charged are not required. Hence the errors due to instrumental constant and tracer charge are avoided. Equation (17) is the relation between tracer response and conversion. However, it is only an implicit form because M_g and Q in the eq. (17) are also a function of conversion. Expressions for M_g and V_g

as a function of conversion have been derived in a previous paper.[12] Hence, M_g and Q in eq. (17) can be given by

$$M_g = M_{gi} + X M_{gx} \tag{18}$$

$$Q = Q_i + X Q_x \tag{19}$$

Substituting eqs. (18) and (19) into eq. (17), one can get the following explicit relation between conversion and tracer response:

$$X = \frac{A(PM_{li}M_b + Q_iK_{bm}M_{vc}) - (P_0M_{l0}M_b + Q_0K_{bm}M_{vc})}{A[P(M_0 + M_{gx})M_b - K_{bm}M_{vc}M_0D_b/(K_{bp}D_p) - Q_xK_{bm}M_{vc}]} \tag{20}$$

where

$$M_{li} = M_0 - M_{gi} - M_{wi}$$

$$M_{l0} = M_0 - M_{g0} - M_{w0}$$

$$Q_0 = \frac{P_0M_b}{RT}(1.0 - W_i)V_r + \frac{W_wM_bP_0}{M_wK_{bw}}$$

$$M_{g0} = \frac{M_{vc}P_{m0}}{RT}(1.0 - W_i)V_r$$

$$M_{w0} = KW_w$$

When $X < X_f$,

$$M_{wi} = M_{w0}$$

$$Q_i = Q_0$$

$$M_{gi} = M_{g0}$$

$$Q_x = \frac{M_bPM_0(1/D_m - 1/D_p)}{RT(1.0 - D_{g0}/D_m)}$$

$$M_{gx} = \frac{M_{vc}P_{m0}M_0(1/D_m - 1/D_p)}{RT(1.0 - D_{g0}/D_m)}$$

When $X \geq X_f$,

$$Q_f = (1.0 - W_i)V_r + X_fM_0(1/D_m - 1/D_p)[1/(1.0 - D_{g0}/D_m) - 1.0]$$

$$Q_i = \frac{PM_bQ_f}{RT} + \frac{W_wM_bP}{M_wK_{bw}}$$

$$M_{gi} = \frac{M_{vc}P_mQ_f}{RT}$$

$$Q_x = \frac{PM_0M_b(1/D_m - 1/D_p)}{RT}$$

$$M_{gx} = \frac{P_mM_0M_{vc}(1/D_m - 1/D_p)}{RT}$$

$$M_{wi} = KW_wP_m/P_{m0}$$

Equation (20) shows that the conversion is an explicit function of tracer response and polymerization conditions over the entire conversion range. This is a general model for the tracer method. If Henry's law constants K_{bm}, K_{bw}, and K_{bp} are given, eq. (20) is ready to be used to calculate the conversion given tracer response and polymerization conditions.

EXPERIMENTAL

To evaluate the model, tracer responses and conversions must be measured and Henry's law constants in the model calculated.

The equipment used for the experiments included a Hewlett Packard (5880 A) Gas Chromatograph with an automatic gas sampler controlled by a microcomputer, and an agitated 5-L stainless steel reactor with a calibrated vacuum-pressure gauge and a thermocouple. The reactor temperature was controlled by a steam and water mixture that circulated in the jacket. The sample flows through the top valve of the reactor and into the GC via a pressure regulator, a rotameter, and a gas sampler. The flow rate of the gas mixture was controlled within 5–7 mL/min at atmospheric pressure.

n-Butane was selected as the tracer, because it is a chemically inert compound (its chain transfer activity is negligible—measurements of molecular weight of PVC with and without *n*-butane were done) and has appropriate vapor pressure; suitable retention time and reasonable distribution among the phases. For a nonreacting mixture system, the reactor was filled with a weighed amount of deionized, distilled water, and a weighted amount of PVC powder. A weighed amount of *n*-butane ($\sim$ 1% based on VCM) and monomer were injected into the reactor, respectively, after the reactor was evacuated. The reactor temperature was then raised progressively to each of the temperature levels used. The concentration of *n*-butane in the vapor phase was determined by GC online. Similarly, for suspension polymerization of VCM, the stabilizer and initiator were charged in the reactor instead of PVC powder. PVC product was weighed to get the conversions. Thus, tracer response and conversion data can be obtained by repeating this procedure. The solubility of *n*-butane in VCM was similarly determined.

PVC used for the present measurements was made using the Rhone Poulenc Bulk Process (Diamond Shamrock/Alberta Gas Company, Fort Saskatchewan, Alberta). VCM was provided by the B. F. Goodrich, Co. (Niagara Falls, Ontario, Canada). Stabilizer, polyvinylalchohol (KP-08) (degree of hydrolysis is 71–75 mol %) and initiator, bis(4-*tert*-butylcyclohexyl) peroxydicarbonate (Perkadox 16-W40) (40% aqueous suspension) were provided by AKZO Chemicals. Azobis(isobutyronitrile) (AIBN) recrystallized was used as an initiator for polymerization at higher temperatures. *n*-Butane (CP grade) was purchased from Canadian Liquid Air Company.

The experimental conditions are as follows:

Preparation of water/VCM/PVC inert mixtures (i.e., nonreacting mixtures):
Reactor volume: 5.0 L
Temperature: 40, 50, 60, 70°C

Initial monomer: 445–1841 g (PVC + VCM in this case)
Water: 2500 g
n-Butane: ~ 1% wt (based on monomer)
Suspension polymerization:
Temperature range: 40–80°C
Initial monomer: 1116 g
Water: 2232 g
Stabilizer: 0.08% wt (based on water)
Initiator: various amount
n-Butane: ~ 1% wt (based on monomer)

The gas chromatograph had a Poropak QS column (80/100 mesh, diameter 3.2 mm length 3.66 m). The analysis conditions were as follows: carrier gas helium, 37.5 mL/min; oven and injection temperature, 150°C; thermal conductivity detector temperature, 200°C.

RESULTS AND DISCUSSION

To calculate the conversions of VCM with eq. (20), we need the area of the tracer response using the vapor mixture sample. Therefore, appropriate operating conditions of GC should be set to clearly separate the peaks for *n*-butane and VCM. Under the present experimental conditions (mentioned above), we obtained the GC response as shown in Figure 1. One can see that there is very good separation between VCM and *n*-butane. According to the retention time of *n*-butane shown in the figure, the run time of GC can be set for 6 min with

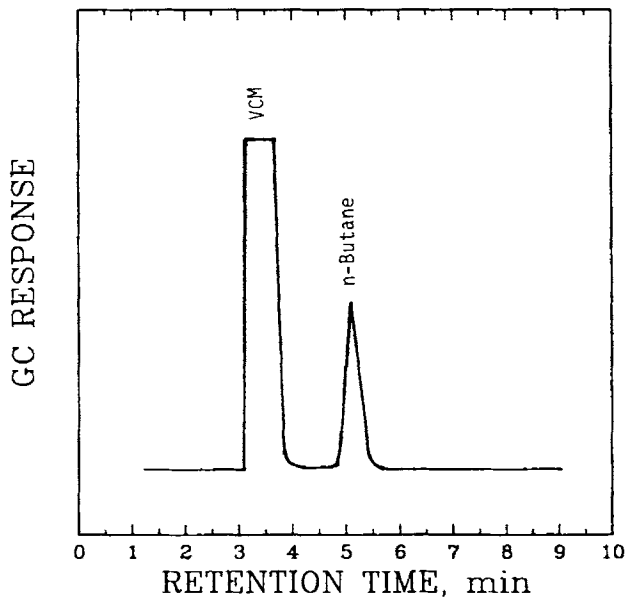

Fig. 1. GC detector responses for vinyl chloride and *n*-butane under the present GC conditions. Retention time: VCM, 3.33 min; *n*-butane, 5.23 min.

the addition of output time for 1 or 2 min. Therefore, the online gas sampler controlled by a microcomputer can automatically sample every 7 or 8 min. This sampling period is adequate for kinetic studies.

There are three Henry's law constants in the model which cannot be estimated independently by using measured conversions and tracer responses. Independent experiments, therefore, must be carried out to obtain these parameters. If two of them are known, the remaining one can be estimated by nonlinear estimation techniques.

Solubility of *n*-Butane in Water and VCM

Extensive data have been published on the solubility of *n*-butane in water.[13] Henry's law constant of *n*-butane in water has been calculated from 12 sources over 15–76.1°C temperature range shown in Figure 2. There is an excellent linear relationship between K_{bw} and temperature. The following correlation was obtained by least squares estimation:

$$K_{bw} = [5.78 - 1580/T\,(\mathrm{K})] \times 10^5 \qquad (\mathrm{atm}) \qquad (21)$$

The solubilities of *n*-butane in VCM and PVC have never been reported. We measured the solubility of *n*-butane in VCM as shown in Figures 3 and 4. The partial pressure of *n*-butane was obtained by determining mole fraction of *n*-butane in the gas phase with GC and total pressure. The mole fraction of *n*-butane in the liquid VCM was obtained by gravimetry. From Figures 3 and 4, one can see that the solubility of *n*-butane in VCM obeys Henry's law within the range of experimental concentrations of interest. The Henry's law constant of *n*-butane in VCM can be obtained using least squares analysis with the data

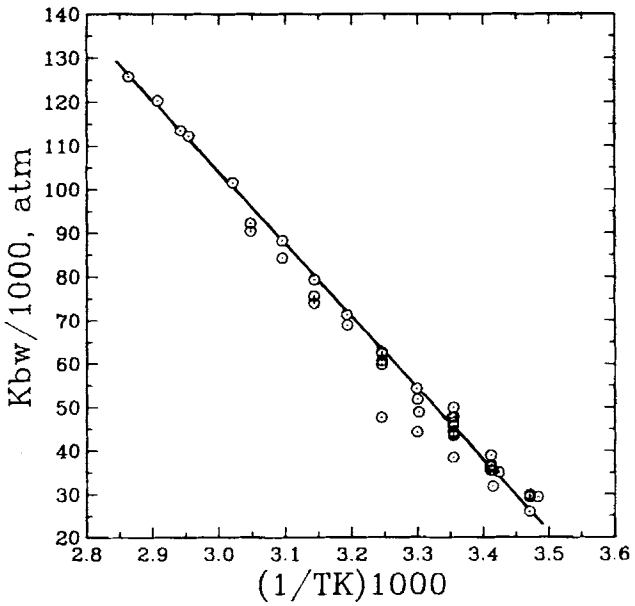

Fig. 2. Henry's law constant for *n*-butane in water versus temperature.

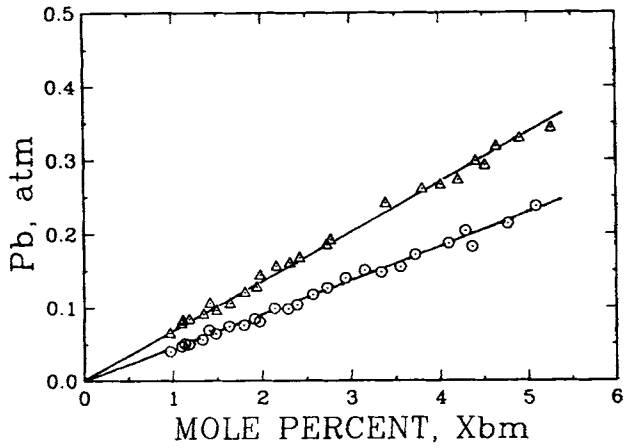

Fig. 3. Solubility of n-butane in vinyl chloride monomer: (⊙) 40°C; (△) 60°C.

shown in the figures. The results are shown in Figure 5. The correlation of K_{bm} with temperature obtained, again, by least squares is the following:

$$K_{bm} = 45.3 - 12800/T\,(\mathrm{K}) \qquad (\mathrm{atm}) \qquad (22)$$

Both K_{bw} and K_{bm} increase with increasing temperature; hence the solubility of n-butane in water and VCM decreases with increasing temperature at the same partial pressure.

Model Evaluation

Once K_{bw} and K_{bm} are known, K_{bp} can be estimated from eq. (20) by nonlinear regression methods. The physical properties of VCM and PVC and critical conversion X_f used in the model are given in a previous paper.[12] The density of n-butane is given by

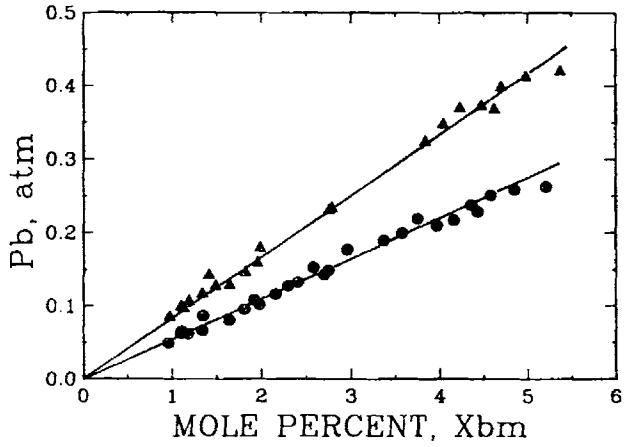

Fig. 4. Solubility of n-butane in vinyl chloride monomer: (●) 50°C; (▲) 70°C.

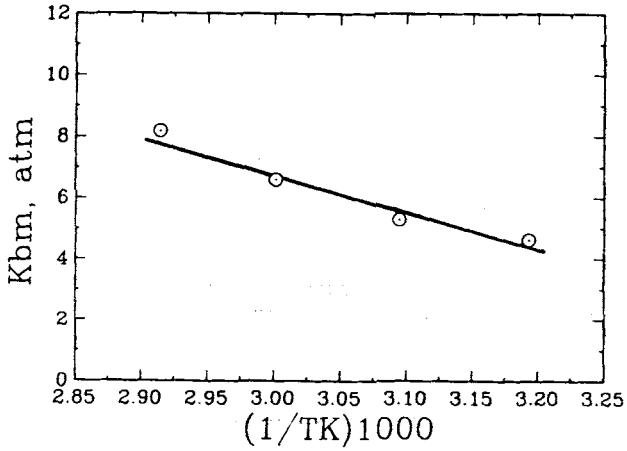

Fig. 5. Henry's law constant for n-butane in vinyl chloride monomer vs. temperature.

$$D_b = 601.7 - 1.14t\ (°C) \qquad (g/L) \tag{23}$$

Equation (23) was obtained from temperature range (0–80°C) data.[14–16]

Inert Mixture System

With inert mixtures of water/VCM/PVC, the solubility constant of n-butane in PVC, K_{bp} was estimated using eq. (20) and a nonlinear regression method. The results are shown in Figure 6. With K_{bp} values, one can notice that the solubility of n-butane in PVC changes dramatically with temperature. Unlike the solubility of n-butane in water and VCM, the solubility in PVC increases with increasing temperature. The correlation between K_{bp} and temperature is given by

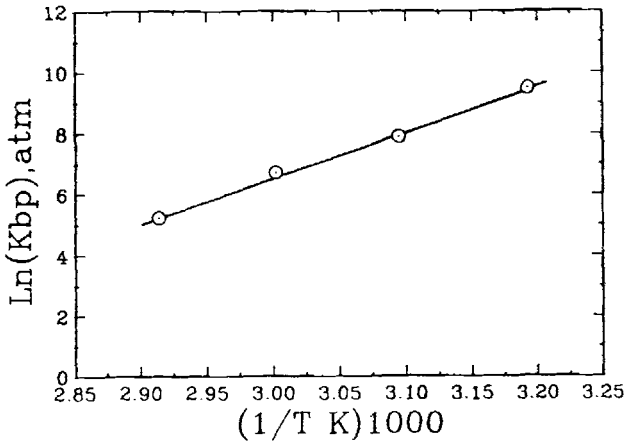

Fig. 6. Apparent solubility constant for n-butane in PVC vs. temperature.

$$K_{bp} = 2.28 \times 10^{-17} \exp(15000/T\,(\mathrm{K})) \quad (\mathrm{atm}) \qquad (24)$$

Using K_{bw}, K_{bm}, and K_{bp} values, one can estimate the concentration of *n*-butane in the different phases. For instance, solubility of *n*-butane in the monomer is about 5 orders of magnitude higher than that in water, and about 2 orders of magnitude higher than that in PVC at 50°C. Therefore, as expected, *n*-butane mainly dissolves in VCM, dissolves slightly in PVC, and hardly dissolves in water.

Using the parameters developed above, knowing the area of the *n*-butane peak measured by GC and the experimental conditions, one can calculate conversions using eq. (20). Typical results are shown in Figure 7. The points are the present experimental data; the solid line is the model prediction. This figure shows that the model is in quite good agreement with experimental data. The standard deviation between experimental data and model predictions for the conversion is within 2–3%. One also can see that the ratio of *n*-butane area is very sensitive to the conversion, particularly at higher conversions. Hence the choice of *n*-butane as the tracer is a good one for the conversion measurements during VCM suspension polymerization.

Suspension Polymerization System

Figure 7 can show that the model is in agreement with the equilibrium data measured using nonreacting mixtures; however, one cannot tell how close to equilibrium one is for conversion measurements during suspension polymerization of VCM. Therefore, it is necessary to carry out VCM suspension polymerizations to reexamine the validity of the parameter K_{bp} estimated using equilibrium data under polymerization conditions. Surprisingly, the conversions calculated by the model with equilibrium K_{bp} are much lower than those measured by gravimetry except in the high conversion range as shown in Figure 8. Therefore, the parameter K_{bp} estimated using inert equilibrium mixtures is not valid for this suspension polymerization system. In other words, for the purpose

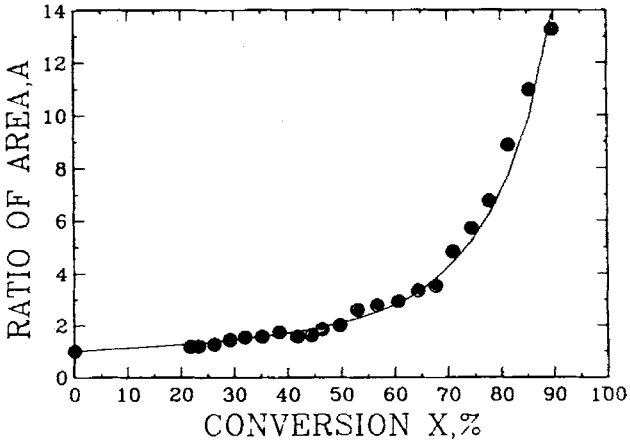

Fig. 7. Ratio of GC detector response area for *n*-butane vs. conversion of VCM at 60°C: (●) experimental data; (—) model prediction.

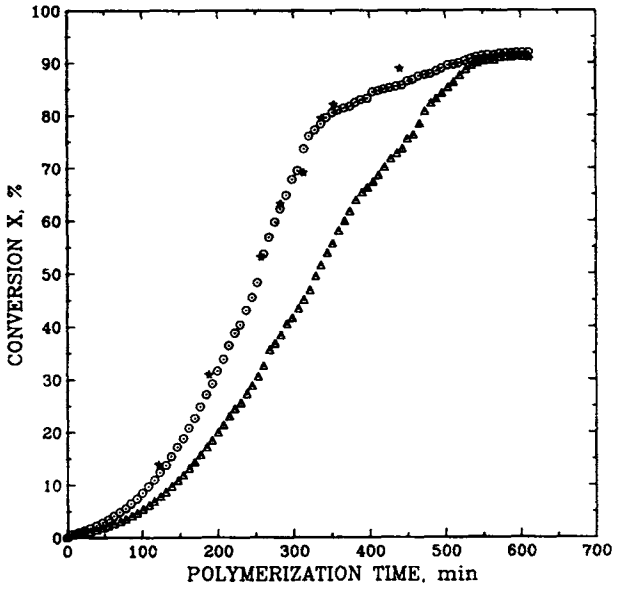

Fig. 8. Comparison between the calibrations based on gravimetry measurements and the equilibrium model for suspension polymerization of VCM at 50°C. Perkadox 16-W40, [I] = 0.15% by wt based on pure peroxide. (⊙) *n*-Butane tracer measurements using parameters obtained via gravimetry measurements; (△) *n*-butane tracer measurements using equilibrium parameters; (★) gravimetry measurements.

of conversion measurements during polymerization, the system must be recalibrated based on gravimetry.

The parameter K_{bp} estimated using suspension polymerization data is much smaller than that found using inert mixtures as shown in Figures 6 and 9. Unlike the inert mixture system, the temperature dependence of K_{bp} for suspension polymerization is nonlinear. The data are best fitted by the following empirical equation:

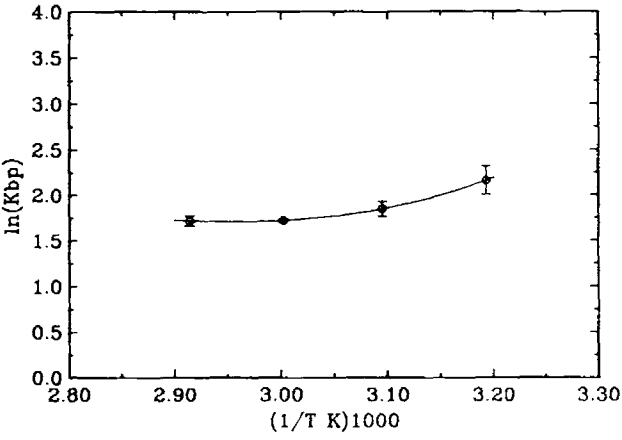

Fig. 9. K_{bp} vs. temperature for suspension polymerization of vinyl chloride (nonequilibrium values measured by gravimetry).

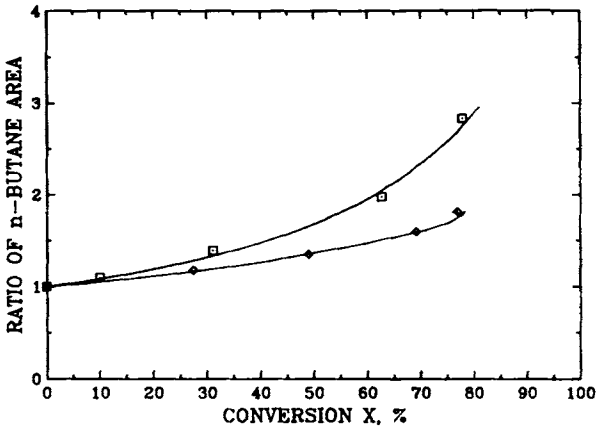

Fig. 10. Ratio of n-butane area versus conversion for suspension polymerization of VCM at 40 and 60°C: (□) at 40°C; (♦) at 60°C; (—) model (with nonequilibrium parameters).

$$\ln(K_{bp}) = a + \frac{b}{T} + \frac{c}{T^2} + \frac{d}{T^3} \tag{25}$$

where $a = -1.73 \times 10^2$, $b = 1.95 \times 10^5$, $c = -7.18 \times 10^7$, and $d = 8.77 \times 10^9$.

The model is in agreement with equilibrium data of inert system over the entire conversion range as shown in Figure 7. However, the model can only fit the data for suspension polymerization system up to about 80% conversion as shown in Figures 10 and 11. The standard deviations between experimental data and model prediction shown in Figures 10 and 11 are within 1–3%.

At higher conversions, the GC responses of n-butane increase dramatically and fall on a single curve for the present experimental temperature range (40–80°C) as shown in Figure 12. The relationship between conversion and ratio of n-butane area can be expressed by the empirical equation as follows:

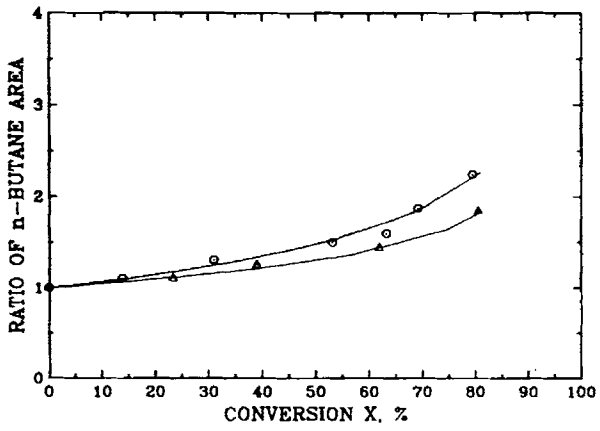

Fig. 11. Ratio of n-butane area versus conversion for suspension polymerization of vinyl chloride at 50 and 70°C: (⊙) at 50°C; (△) at 70°C; (—) model (with nonequilibrium parameters).

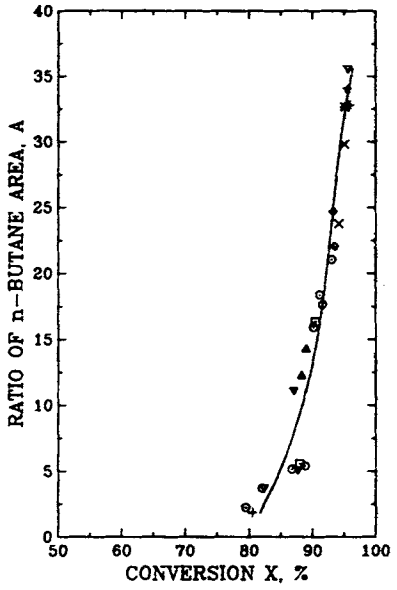

Fig. 12. Ratio of n-butane area versus conversions for suspension polymerization of vinyl chloride at higher conversion stage: (△) 40°C; (□) 45°C; (⊙) 50°C; (◇) 55°C; (×) 60°C; (▽) 65°C; (+) 70°C; (★) 75°C; (∗) 80°C; (—) empirical calibration curve [eq. (28)].

$$X = 79.5 + 1.25A - 4.24 \times 10^{-2}A^2 + 5.76 \times 10^{-4}A^3 \qquad (26)$$

where the constants were estimated by a nonlinear regression.

With the model using parameters estimated using gravimetry and the empirical equation (26), one can recalculate the conversion histories of suspension polymerization of VCM over the entire conversion range for the same run as shown in Figure 8. One can see, in Figure 8, that the model with parameters based on gravimetry measurements is in excellent agreement with conversions measured by gravimetry.

From Figures 7–12, one can see that the suspension polymerization system of vinyl chloride is quite different from the inert mixture system in terms of the GC responses of n-butane. This disagreement is likely due to nonequilibrium effects. The reaction system may not reach equilibrium and therefore the GC response for n-butane is much lower in the reaction system than in the inert system. The morphology of PVC may play an important role in this regard. With increasing conversion, the particles of PVC experience several structural transition stages.[17] The solubility as well as the diffusion coefficient may depend on the morphology of PVC. At high conversions, the liquid monomer phase has been consumed, and monomer in the vapor phase diffuses into the polymer phase and n-butane diffuses from the polymer phase into the vapor phase so that the concentration of n-butane in the vapour phase increases. In the meantime, the monomer concentration in the polymer phase decreases dramatically due to polymerization so that the solubility of n-butane in the polymer phase decreases. As a result, the GC response of n-butane increases dramatically at high conversions.

To further evaluate the model, a series of experiments with higher water/VCM ratios and lower initiator concentrations were done at AKZO Chemicals. The experimental procedure used by AKZO is similar to that used at MIPPT except that a lower heating rate to polymerization temperature was employed. The heating time was about 60 min at AKZO and about 5 min at MIPPT. Slower heating rates and lower initiator concentrations permit the polymerization system to approach equilibrium with respect to *n*-butane diffusion. The results are shown in Figure 13. The solid curve is the model prediction with equilibrium-based parameters. The experimental points were obtained by stopping the polymerization at different conversion levels and weighing the dried PVC. It should be pointed out that the model predictions for the different temperatures overlap. One can see that the experimental data also give essentially one graph under these experimental conditions. The model is in excellent agreement with the experimental data up to 60% conversion. At higher conversions, the model predictions are lower than experimental measurements by gravimetry. These results suggest that the equilibrium model can be used to estimate conversions when polymerizations are relatively slow.

Precision of the Tracer Method

As mentioned above, the ratio of *n*-butane area is used in the model instead of area. It is essential, therefore, to obtain an accurate initial area for *n*-butane

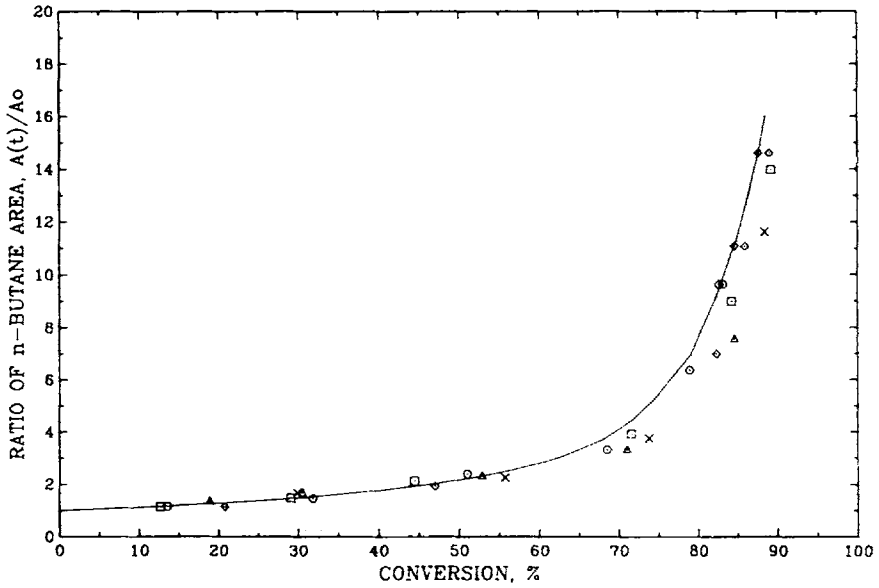

Fig. 13. Comparison of equilibrium model predictions with gravimetry measurements done by AKZO Chemicals. Reactor: 5.0 L, water: 2700 g, VCM: 675 g. (—) Equilibrium model; (⊙) initiator: α-cumyl-peroxyneodecanoate (Trigonox-99), [I] = 0.15% by wt based on pure peroxide, at 42°C; (△) initiator: dimyristyl peroxydicarbonate (Perkadox-26), [I] = 0.085% by wt based on pure peroxide, at 53.5°C; (□) initiator: dimyristyl peroxydicarbonate (Perkadox-26), [I] = 0.060% by wt based on pure peroxide, at 57°C; (◈) initiator: bis(4-*tert*-butylcyclohexyl) peroxydicarbonate (Perkadox 16-W40), [I] = 0.060% by wt based on pure peroxide, at 62°C; (×) initiator: dilauroyl peroxide (Laurox), [I] = 0.15% by wt, at 62°C.

for later conversion calculations. Unfortunately, it is very difficult to obtain accurate A_{b0} experimentally because of system noise at the beginning of the polymerization. In fact, the n-butane area often decreases for a starting period at the beginning of the polymerization. This phenomenon was observed at both MIPPT and AKZO laboratories. To obtain A_{b0} accurately, the following empirical equation was used to smooth the experimental data:

$$A_b = A_{b0} + A_1 t + A_2 t^2 + A_3 t^3 \tag{27}$$

A typical response of n-butane for VCM suspension polymerization is shown in Figure 14. With this technique, one cannot only estimate A_{b0} satisfactorily for each run but also smooth the original data. The scattering due to experimental noise, therefore, is avoided.

Figures 15 and 16 show the replicate experiments for conversion measurements by the tracer technique. One can see that the reproducibility of conversion histories of VCM polymerization are quite satisfactory. The maximum deviations appear in the conversion range 50–80%. The average variances and standard deviations corresponding to data in Figures 15 and 16 are shown in Table I. One can see, from Table I, that the standard deviation is within 2% conversion, which indicates a good precision of the present tracer method.

Figure 17 shows conversion–time histories for the suspension polymerization of vinyl chloride as measured by the n-butane-tracer method with calibration based on gravimetry. The final points (stars) were obtained by point gravimetry measurements as a check. The errors for final conversions measured by tracer method and gravimetry are less than 1%. The conversion data using the tracer method are very smooth over the entire conversion range. With the tracer

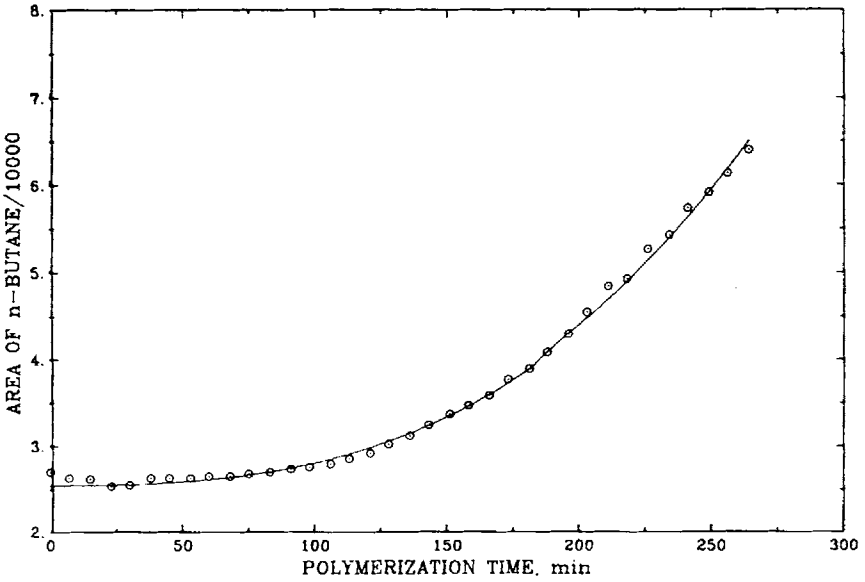

Fig. 14. Area of n-butane vs. reaction time for suspension polymerization of VCM at 60°C; (⊙) experimental data; (—) best fit curve.

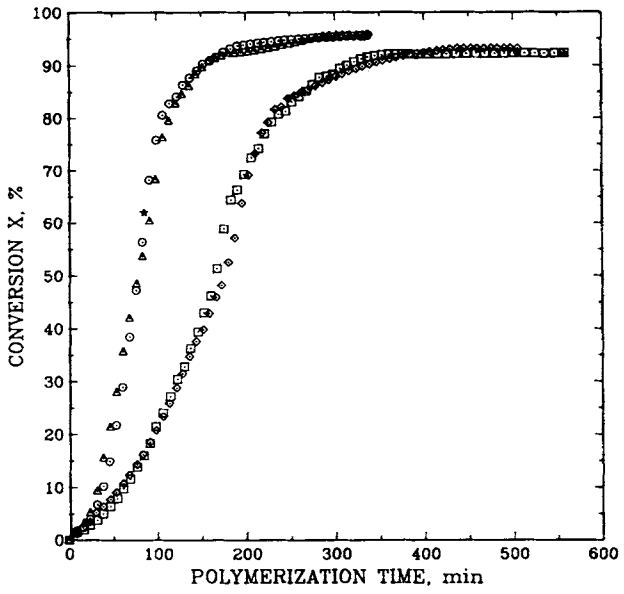

Fig. 15. Reproducibility of conversion histories for suspension polymerization of VCM measured by the n-butane tracer method: (⊙ and △) at 70°C, AIBN, [I] = 0.25% by wt; (□ and ◇) at 50°C, Perkadox 16-W40, [I] = 0.20% by wt based on pure peroxide; (★) measured offline by gravimetry.

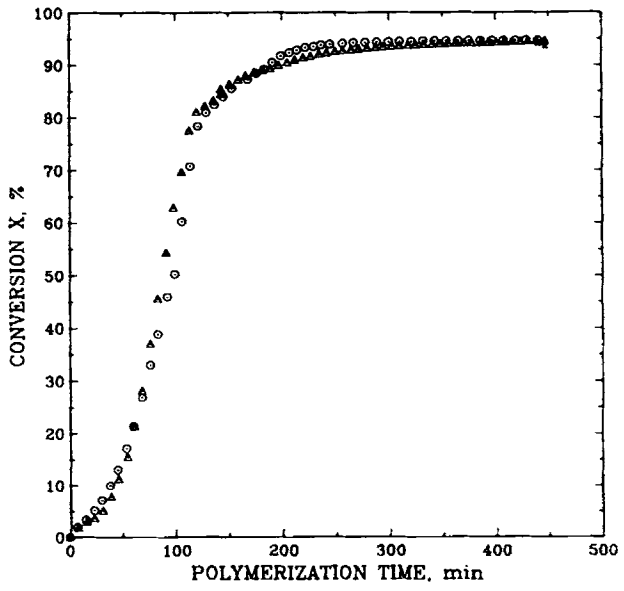

Fig. 16. Reproducibility of conversion histories for suspension polymerization of VCM measured by the n-butane tracer method. Perkadox 16-W40, [I] = 0.175% by wt based on pure peroxide, at 60°C.

TABLE I
Reproducibility of Conversion Measurements by the Tracer Technique

Temp (°C)	Average variance	Average standard deviation	Degree of freedom
50	1.7	1.3	68
60	2.3	1.5	60
70	3.0	1.7	45

method, one can get very detailed kinetic information. One can easily estimate the instantaneous polymerization rate every 7–8 min as shown in Figure 18. However, we will not discuss the kinetic behavior of VCM polymerization at the present time. This will be done in a future publication.

As mentioned above, the sample flow rate of headspace vapor was controlled within 5–7 mL/min at atmospheric pressure. Therefore, for a long run, say, 10 h, the losses of material due to sampling is less than 10 g. For the present reactor charge (1116 g VCM), the relative error due to sampling is less than 1%. Therefore, under the present operating conditions, the error due to sampling can be neglected.

Because all the parameters are available as a function of temperature and other variables in eq. (20) are a function of polymerization conditions, this model can be used not only for isothermal batch polymerization but also for nonisothermal and semibatch polymerizations.

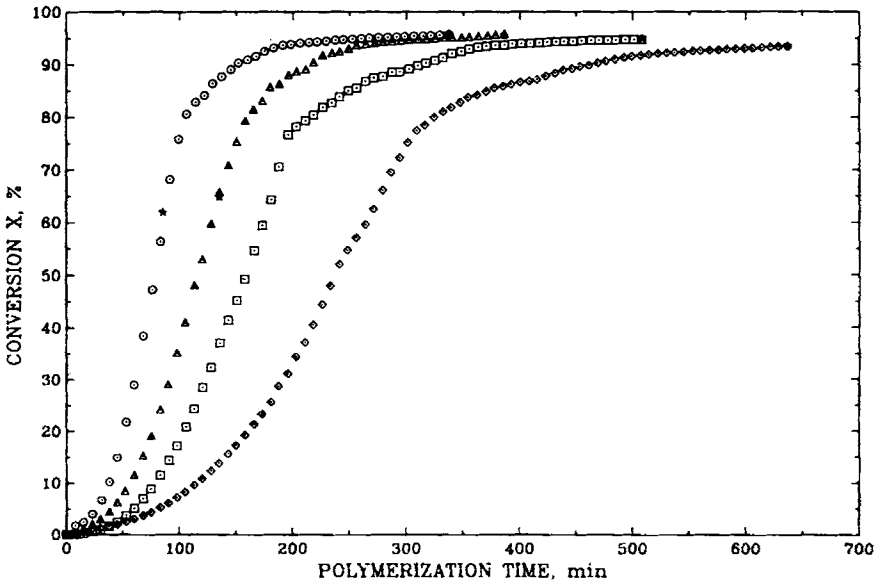

Fig. 17. Typical conversion histories for the suspension polymerization of VCM measured by the *n*-butane method. Initiator: AIBN, [I] = 0.25% by wt. (⊙) 70°C; (△) 65°C; (□) 60°C; (◇) 55°C.

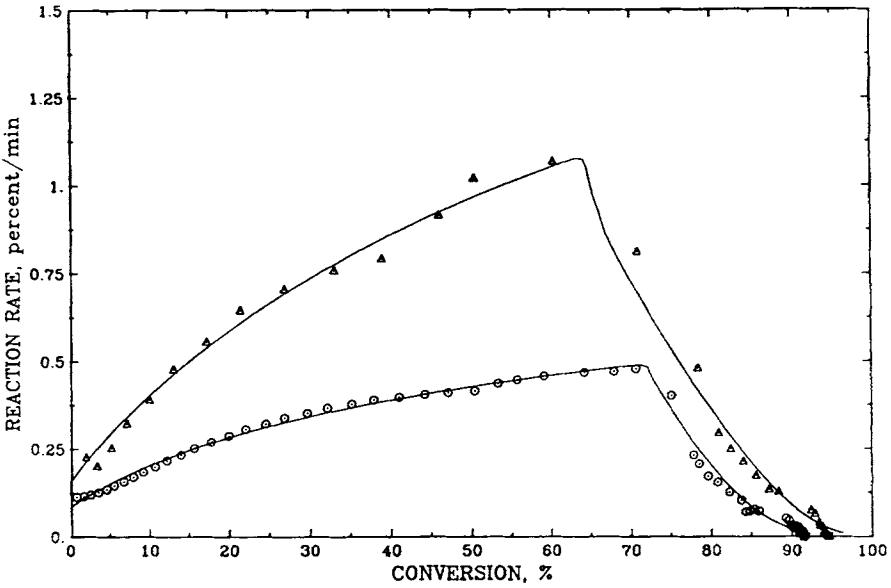

Fig. 18. Polymerization rate variation with conversion for suspension polymerization of VCM. Initiator: Perkadox 16-W40, [I] = 0.175% by wt based on pure peroxide. (△) 60°C; (⊙) 50°C; (—) kinetic model.

Compared with gravimetry, the present method has the following advantages: It has higher efficiency, is safer, is more flexible for different reactor processes, and more detailed kinetic information can be obtained. The calculation procedure is, however, more complicated than that for gravimetry. However, with the use of computer, only a few seconds are required to calculate a hundred pairs of conversion data with the present model.

CONCLUSIONS

The present calibration for the *n*-butane tracer method model theoretically relates monomer conversion to tracer response measured by gas chromatography. The tracer *n*-butane has an appropriate retention time with good separation from VCM under the present experimental conditions. The partition of *n*-butane between the different phases meets the requirements of the tracer method. The detector response of *n*-butane is very sensitive to the conversion of VCM, particularly at high conversions. The model is in reasonable agreement with the experimental results over the entire conversion range when equilibrium is closely followed, and it is in agreement with the experimental results up to limiting conversion (glassy-state transition) for fast suspension polymerization when nonequilibrium calibration parameters are used. The model can be used not only for isothermal batch but also for nonisothermal batch, and semibatch polymerization. The sampling period under the present experimental conditions is adequate for kinetic studies of VCM polymerization.

Financial support from the Natural Science and Engineering Research Council and the McMaster Institute for Polymer Production Technology is appreciated. The assistance of P. Gloor, D. Keller, D. Anderson, H. Li, and N. Ali is gratefully acknowledged.

APPENDIX: NOMENCLATURE

A the ratio of tracer response area at conversion X to zero conversion
A_b area of tracer response at conversion X
A_{b0} area of tracer response at zero conversion
B total mass of tracer (g)
B_g mass of tracer in the gas phase (g)
B_m mass of tracer in the monomer (g)
B_p mass of tracer in the polymer (g)
B_w mass of tracer in the water (g)
D_b density of n-butane (g/L)
D_{g0} density of VCM vapour under the vapour pressure (g/L)
D_m density of monomer (g/L)
D_p density of polymer (g/L)
D_w density of water (g/L)
f_i fugacity of tracer in the different phases (atm)
K solubility constant of VCM in water
K_b proportional constant
K_{bm} Henry's law constant of tracer in monomer (atm)
K_{bp} apparent solubility constant of tracer in PVC (atm)
K_{bw} Henry's law constant of tracer in water (atm)
M_0 initial monomer charged (g)
M_g mass of monomer in the gas phase (g)
M_b molecular weight of tracer (g)
M_{vc} molecular weight of VCM (g)
M_w molecular weight of water (g)
M_{wi} mass of monomer in water phase (g)
P the total pressure (atm)
P_b the partial pressure of n-butane (atm)
P_m the partial pressure of monomer (atm)
P_{m0} the vapour pressure of monomer (atm)
P_0 the initial total pressure of the system (atm)
Q a variable used in the model
R gas constant (atm, 1/mol, K)
t temperature (°C)
T absolute temperature (K)
V_g volume of the gas phase (L)
V_r reactor volume (L)
W_i the fraction of initial reactor charge as liquid
W_w mass of water charged (g)
X conversion of monomer
X_{bm} mole fraction of tracer in monomer, tracer free basis
X_{bp} volume fraction of tracer in PVC, tracer free basis
X_{bw} mole fraction of tracer in water, tracer free basis
X_f critical conversion
Y_b mole fraction of tracer in the vapor phase

Subscripts

m monomer
p polymer
w water
0 initial

References

1. W. I. Bengough and R. G. W. Norrish, *Proc. Royal Soc. (Lond.) A*, **200**, 301 (1950).
2. E. Farber and M. Koral, *Polym. Eng. Sci.*, **8**, 11 (1968).

3. A. Crosato-Arnaldi, P. Gasparini, and G. Talamini, *Makromol. Chem.*, **117,** 140 (1968).
4. A. H. Abdel-Alim and A. E. Hamielec, *J. Appl. Polym. Sci.*, **16,** 783 (1972).
5. T. Y. Xie, Z. Z. Yu, Q. Z. Cai, and Z. R. Pan, *J. Chem. Ind. Eng. (China)*, **2,** 93 (1984).
6. V. P. Malhotra and U. K. Saroop, *Pop. Plast.*, **29,** 17 (1984).
7. M. R. Meeks, *Polym. Eng. Sci.*, **9,** 141 (1969).
8. H. Nilsson, G. Silvegren, and B. Törnell, *Br. Polym. J.*, **13,** 164 (1981).
9. H. Nilsson, C. Silvegren, and B. Törnell, *Chem. Scripta,* **19,** 164 (1982).
10. H. Nilsson, C. Silvegren, and B. Törnell, *Angew. Makromol. Chem.*, **112,** 125 (1983).
11. M. Langsam, *J. Polym. Sci. Polym. Lett. Ed.*, **22,** 549 (1984).
12. T. Y. Xie, A. E. Hamielec, P. E. Wood, and D. R. Woods, *J. Appl. Polym. Sci.*, **34,** 1749 (1987).
13. W. Hayduk, *IUPAC Solubility Data Ser.*, **24,** 16 (1986).
14. R. C. Weast, M. J. Astle, and W. H. Beyer, Eds., *CRC Handbook of Chemistry and Physics*, 64th ed., CRC Press, Boca Raton, FL, 1983–1984.
15. *Selected Values of Properties of Hydrocarbons and Related Compounds*, American Petroleum Institute Research Project 44 (API 44), 1969, Vols. 1 and 2.
16. R. W. Gallant, *Hydrocarbon Process. Pet. Refiner,* **44,** 95 (1965).
17. T. Y. Xie, A. E. Hamielec, P. E. Wood, and D. R. Woods, paper presented at the Akzo Chemie PVC Symposium 1988, The Netherlands.

Received July 14, 1989
Accepted February 15, 1990